Theoretical evidence and chemical origin of the magnetism-dependent electrostructural coupling in La_2NiMnO_6

Hena Das,[1] Umesh V. Waghmare,[2,*] T. Saha-Dasgupta,[1,†] and D. D. Sarma[3,4]
[1]*S.N. Bose National Centre for Basic Sciences, Kolkata 700098, India*
[2]*Jawaharlal Nehru Centre for Advanced Scientific Research, Jakkur, Bangalore-560064, India*
[3]*Centre for Advanced Materials, Indian Association for the Cultivation of Science, Jadavpur, Kolkata 700032, India*
[4]*Solid State and Structural Chemistry Unit, Indian Institute of Science, Bangalore 560012, India*
(Received 22 December 2008; revised manuscript received 8 March 2009; published 3 April 2009)

Using first-principles density-functional calculations, we determine and analyze the Born effective charges Z^* that describe the coupling between electric field and atomic displacements for ferromagnetic double-perovskite compound, La_2NiMnO_6. We find that the Born effective charge matrix of Ni in La_2NiMnO_6, has an anomalously large antisymmetric component, whose magnitude reduces substantially upon change in the magnetic ordering between Ni and Mn, showing it to be a magnetism-dependent electrostructural coupling. We use a local picture of the electronic structure obtained with Wannier functions, along with its band-by-band decomposition to determine its electronic origin.

DOI: 10.1103/PhysRevB.79.144403 PACS number(s): 71.15.Mb, 71.20.−b, 77.22.−d

I. INTRODUCTION

There has been a surge of interest in materials exhibiting magnetoelectric couplings, such as $CdCr_2S_4$,[1] multiferroic $BiMnO_3$,[2] and Bi_2NiMnO_6.[3] Recently, La_2NiMnO_6,[4] a ferromagnetic (FM) insulator in the ordered double-perovskite structure, was shown to exhibit a room-temperature magnetocapacitance, a coupling between magnetization, and electric polarization. A recent calculation[5] showed that it is possible to drive this compound ferroelectric by alloying with Lu at La site, giving rise to simultaneous presence of two order parameters: ferromagnetism and ferroelectricity. While such materials have tremendous potential for technological applications, they are relatively rare and it is fundamentally interesting to understand microscopic mechanisms behind their properties.

La_2NiMnO_6 (LNMO) occurs in a distorted double-perovskite structure with a high-temperature phase with rhombohedral symmetry [see Fig. 1(a)]. The magnetic-susceptibility measurements of La_2NiMnO_6 (LNMO) in an applied magnetic field of 1 T show a magnetic transition[4] at $\approx$280 K, demonstrating the onset of ferromagnetic long-range ordering in an insulating compound at a temperature as high as about room temperature. Further, its dielectric constant[4] measured as a function of temperature exhibits a jump at T_{jump}. The temperature T_{jump} shifts toward the ferromagnetic transition temperature upon application of a small magnetic field, indicating the near room-temperature magnetocapacitive behavior of the compound. Most of the dielectric response of LNMO was found to arise from its low-energy IR-active optical phonons, which were shown to couple strongly with its magnetic order.[6]

Dielectric response of a phonon is determined primarily by its frequency and the electric-dipole moment p. The latter is given by the Born effective charge[7] (BEC) tensor $Z^*_{\kappa,\alpha\beta}$ through the relationship:

$$p_\alpha = Z^*_{\kappa,\alpha\beta}\tau_{\kappa,\beta},$$

where $\tau_{\kappa,\beta}$ is the movement of an ion κ along the direction β. Physically, Z^* measures the microscopic current flowing across the sample while the ions are adiabatically displaced. Such currents are responsible for building up the spontaneous polarization when ions are displaced from the centrosymmetric position to the ferroelectric structure.[8]

In another physical interpretation, it gives the force F the ion feels in direction α through interaction with electric field E in direction β,

$$F_{\kappa,\alpha} = Z^*_{\kappa,\alpha\beta}E_\beta.$$

Z^* is therefore a measure of the strength of electrostructural coupling of an insulating material. Being related to dynamical changes of the hybridization between various ions,[9] values of Z^* are often found to be highly nontrivial and can reach values twice as large as the static nominal ionic changes. While in simple high-symmetry insulators, the Z^* matrix is typically isotropic with only nonzero identical diagonal components for a general case Z^* can have both diagonal and off-diagonal components which need not to be even symmetric.

In the following, we report density-functional-theory (DFT) -based first-principles investigation of the Born effective charges of LNMO in the high-temperature rhombohedral symmetry identifying its microscopic origin. Our computed Born effective charges for LNMO show presence of large off-diagonal components at the Ni site, which are totally antisymmetric and sensitive to changes in magnetic ordering between Ni and Mn. The work by Massidda *et al.*[10] in this context carried out for transition-metal monoxides showed the effect of magnetic anisotropy on Z^* in terms lowering of symmetry of the magnetic space group; while in the current example, as elaborated in the following, the magnetic ordering changes the hybridization and therefore influences the magnitude of the components of Z^* without effecting the symmetry. The effect described in the following is therefore of different origin than what has been described in Ref. 10 and to best of our knowledge has not been reported previously. We note that while change of the coordinate system can change the tensor elements of Z^* as discussed in Ref. 11

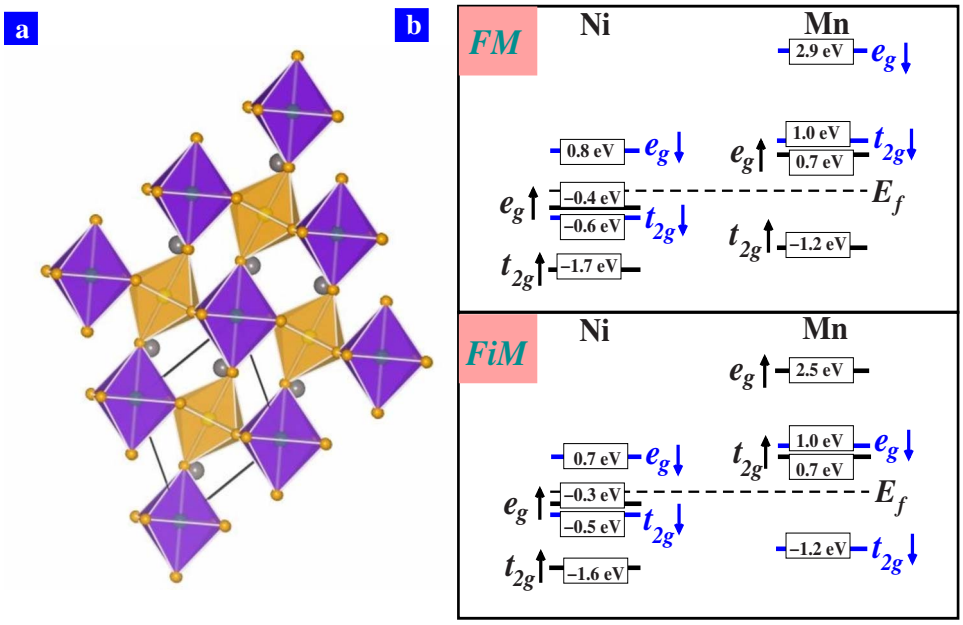

FIG. 1. (Color online) (a) Crystal structure viewed along the pseudocubic [111] direction revealing the high-temperature rhombohedral structure of La_2NiMnO_6. The violet (dark gray) and orange (light gray) colored octahedra denote the NiO_6 and MnO_6 octahedra, respectively. The La atoms shown as big balls sit in the hollow formed by NiO_6 and MnO_6 octahedra. The NiO_6 and MnO_6 octahedra connected by corner sharing O atom are tilted with respect to each other. The Ni, Mn, and the connecting O atoms therefore do not sit in a straight line; rather they form a triangle with Ni-O-Mn angle of 157°. (b) Energy level positions of Ni and Mn *d* levels with respect to Fermi energy E_f as obtained in DFT calculation. The upper (lower) panel corresponds to ferromagnetic (ferrimagnetic) spin arrangement between Ni and Mn spins.

the totally antisymmetric part of Z^*, as observed for LNMO, does not change under similarity (coordinate) transformation and therefore reflects the fundamental property of the material.

The rest of the paper is organized in the following manner. Section II is devoted to brief description of the computational techniques employed in the work. Section III provides the main result of the paper, namely the Born effective charges of LNMO. In Sec. IV, we attempt on a microscopic understanding of the calculated Born effective charges. Section V discusses the comparison with other compounds. Section VI concludes the paper.

II. METHODOLOGY

The computation of Born effective charges has been carried out with the plane-wave pseudopotential method as implemented in the ABINIT code.[12] We used a spin polarized generalized gradient approximation (GGA) (Ref. 13) to the exchange-correlation functional. The wave functions were expanded in the plane-wave basis with a kinetic-energy cutoff of 80 Ryd. Reciprocal space integration was carried out with a *k* mesh of $5\times5\times5$.

In order to gain insights on the electronic origin of computed Born effective charges, we have employed the muffin-tin orbital (MTO) based *N*th order MTO-downfolding technique.[14] This technique creates few-band Hamiltonians out of a full DFT Hamiltonians through energy-selective procedure of integrating out degrees of freedom. If the chosen low-energy bands form an isolated set of bands, as in the example of transition-metal *d* states of LNMO, the underlying orbitals span the same Hilbert space of the corresponding Wannier functions, giving rise to Wannier functions generated a direct manner. Such technique has been employed in past in generation of Wannier functions in high-T_c cuprates,[15] in pyrochlore compound $Tl_2Mn_2O_7$ (Ref. 16) and in low-dimensional quantum spin systems.[17] The accuracy of the NMTO calculation has been checked through a comparison with plane-wave calculations.

Further, we have carried out the analysis of the contribution of the different set of bands to the BECs of different ions, a technique known as band-by-band decomposition.[18] In this technique, individual contributions are obtained by considering the Bloch functions associated with a particular set of bands as elements of overlap matrix.

III. BORN EFFECTIVE CHARGES IN LA_2NIMNO_6

Our calculated BECs of La, Ni, and Mn (shown in Table I) follow the rhombohedral site symmetry, with a threefold axis along pseudocubic [111] direction, while that at the O site is lowered, leading to strong anisotropy of the oxygen Z^* tensor. We find anomalously large charges at Mn site (+6–+7, significantly larger compared to its nominal valence of +4), similar to earlier report on $CaMnO_3$.[19] The striking feature appears in the Born effective charges of Ni, which show anomalously large *antisymmetric* off-diagonal components in the Born effective charge matrix, though the diagonal elements have a value close to the nominal charge of Ni(+2). More interestingly we found that the largeness of these anti-

TABLE I. Calculated Born effective charge tensors at the La, Ni, Mn, and O sites of La_2NiMnO_6 at FM and FiM phases. Note the presence of large off-diagonal elements which are antisymmetric specially in case of Ni. Changing the magnetic ordering between Ni and Mn from FM to FiM has profound effect in terms of making the antisymmetric off-diagonal components at Ni weaker.

	Ferromagnetic	Ferrimagnetic
$Z^*_{La}{}^{(T)}$	$\begin{pmatrix} 4.52 & 0.0 & 0 \\ 0.0 & 4.52 & 0 \\ 0 & 0 & 4.38 \end{pmatrix}$	$\begin{pmatrix} 4.57 & -0.11 & 0 \\ 0.11 & 4.57 & 0 \\ 0 & 0 & 4.31 \end{pmatrix}$
$Z^*_{Ni}{}^{(T)}$	$\begin{pmatrix} 2.48 & 3.23 & 0 \\ -3.23 & 2.48 & 0 \\ 0 & 0 & 2.24 \end{pmatrix}$	$\begin{pmatrix} 2.03 & 1.22 & 0 \\ -1.22 & 2.03 & 0 \\ 0 & 0 & 1.64 \end{pmatrix}$
$Z^*_{Mn}{}^{(T)}$	$\begin{pmatrix} 6.44 & -0.37 & 0 \\ 0.37 & 6.44 & 0 \\ 0 & 0 & 6.52 \end{pmatrix}$	$\begin{pmatrix} 7.51 & -0.98 & 0 \\ 0.98 & 7.51 & 0 \\ 0 & 0 & 6.54 \end{pmatrix}$
$Z^*_{O1}{}^{(T)}$	$\begin{pmatrix} -3.70 & -0.48 & 0.91 \\ 0.48 & -2.28 & -0.35 \\ 0.91 & 0.35 & -2.92 \end{pmatrix}$	$\begin{pmatrix} -3.67 & 0.21 & 0.93 \\ 0.21 & -2.54 & -0.22 \\ 1.01 & -0.18 & -2.80 \end{pmatrix}$
$Z^*_{O2}{}^{(T)}$	$\begin{pmatrix} -2.64 & 0.14 & -0.15 \\ 1.09 & -3.35 & 0.97 \\ -0.76 & 0.62 & -2.92 \end{pmatrix}$	$\begin{pmatrix} -2.64 & 0.38 & -0.28 \\ 0.38 & -3.59 & 0.92 \\ -0.35 & 0.97 & -2.80 \end{pmatrix}$
$Z^*_{O3}{}^{(T)}$	$\begin{pmatrix} -2.64 & -1.09 & -0.76 \\ -0.14 & -3.35 & -0.62 \\ -0.15 & -0.97 & -2.92 \end{pmatrix}$	$\begin{pmatrix} -3.03 & -0.60 & -0.65 \\ -0.60 & -3.21 & -0.70 \\ -0.66 & -0.79 & -2.80 \end{pmatrix}$

symmetric off-diagonal components depend sensitively upon the magnetic ordering between Ni and Mn. While the change in magnetic ordering from FM to ferrimagnetic (FiM) state affects almost all the matrix elements of Born effective charge tensor, the most significant change occurs in the off-diagonal component of the Born effective charge of Ni. This implies that the anomalous and antisymmetric Born effective charge of Ni is intimately connected with the magnetic coupling between Ni and Mn, *thereby giving rise to a magnetism-dependent electrostructural coupling*.

We note that the Z^* of oxygen atoms also undergo interesting changes due to their hybridization with metal ions. The antisymmetric components of Z^* of oxygen atoms weaken (almost vanishes) significantly in the FiM state relative to FM one. Focusing on to Mn, we find that both diagonal and off-diagonal antisymmetric components are enhanced in the FiM phase compared to that in FM phase.

IV. ELECTRONIC ORIGIN

We now turn to determine the electronic origin of these anomalous antisymmetric charges. We first summarize, the salient features of the electronic structure of double-perovskite compound LNMO as found in earlier communications.[5,6] The transition-metal ions Ni and Mn in $d^8(2+)$ and $d^3(4+)$ configurations are octahedrally surrounded by oxygen atoms. This causes crystal-field splitting of Ni and Mn d states into t_{2g} and e_g symmetries. The presence of finite magnetic moments at both Ni and Mn sites also causes spin splitting of t_{2g} and e_g states. Ni being in d^8 state and in $S=1$ spin configuration, both t_{2g} and e_g states in the majority-spin channel are filled while only the t_{2g} states are occupied in the minority-spin channel. In the spin $S=3/2$ configuration of Mn ion, only t_{2g} states are fully occupied in the majority-spin channel, and both t_{2g} and e_g states remain empty in the minority-spin channel. The energy-level positions of Ni and Mn d states in the ferromagnetic and ferrimagnetic alignment of Ni and Mn spins, as obtained in DFT calculations within the framework of GGA, are shown in the upper and lower panels of Fig. 1(b). The insulating solution is obtained for both FM and FiM phases in the DFT-GGA calculations with the Fermi energy lying in the gap between Ni e_g(Ni t_{2g}) and Mn e_g(Mn t_{2g}) states in the majority (minority) spin channel for FM phase and between Ni e_g(Ni t_{2g}) and Mn t_{2g}(Mn e_g) states in the majority (minority) -spin channel for FiM phase. The hybridization between Ni and Mn mediated by oxygen with a superexchange mechanism allows only the states of same symmetry and spin to interact.

To understand the microscopic origin of anomalous behavior of Born effective charge, we have constructed Wannier functions corresponding to Ni and Mn d energy bands using NMTO-downfolding technique[14] which involves integrating out degrees of freedom expect for the d- orbitals of Ni or Mn. The constructed Wannier functions have the central symmetry as that of Ni or Mn d orbitals while the tails are shaped according to the symmetries of the integrated out orbitals, which is O p and Mn or Ni d states. Previous work[9] in connection with contributions of change in hybridization to the anomalous charge has shown that it originates primarily from a modification of the interactions between occupied and unoccupied electronic states. Examination of level diagram [Fig. 1(b)] reveals that such situation arises in case of interaction between Ni t_{2g} and Mn t_{2g} symmetries, with Ni t_{2g} states being filled and Mn t_{2g} states being empty for the minority-spin channel in ferromagnetic case and for the majority-spin channel in case of ferrimagnetic spin alignment. Similarly it arises between Ni e_g and Mn e_g symmetries, with Ni e_g states being filled and Mn e_g states being empty for the majority-spin channel for both ferromagnetic and ferrimagnetic cases.

We examine one of the Wannier functions centered on Ni and having t_{2g} symmetry in minority (majority) spin channel for the ferromagnetic (ferrimagnetic) phase for two cases: (a) equilibrium rhombohedral structure and (b) a structure distorted with Ni displaced by 1% of the lattice constant along the crystallographic x axis (see Fig. 2). We notice the central $y'z'$ symmetry, defined in the local coordinate system with z' axis pointing along one of the Ni-O bond, while the tails in the immediate neighborhood are shaped according to oxygen $p_{y'}$ and $p_{z'}$ orbitals which form antibonds with the central Ni $y'z'$ symmetry. The end of these tails consist of t_{2g} orbitals (largely unoccupied) of the next-nearest-neighbor Mn atoms, leading to a finite mixing of orbitals of Ni and Mn. The effective Ni-centered Wannier function is longer ranged in

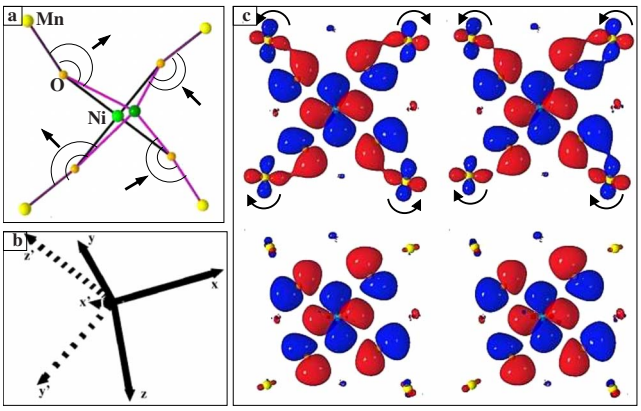

FIG. 2. (Color online) (a) Atomic structure of La_2NiMnO_6 in the equilibrium configuration compared to the structure where Ni atom has been moved along the rhombohedral x axis. The green, yellow and orange balls mark the positions of Ni, Mn, and O atoms. The lighter and darker green balls indicate the positions of Ni at equilibrium and that after displacement. The movement of Ni atom strongly influences the $\angle$Ni−O−Mn, increasing it one quadrant and decreasing it in the opposite quadrant from the equilibrium $\angle$Ni−O−Mn. (b) The rhombohedral global coordinate system and the oxygen-based octahedral coordinate system. The unprimed and primed coordinate systems represent the rhombohedral coordinate system (z axis pointing along the pseudocubic [111] direction) and the oxygen-based octahedral coordinate system (z' axis pointing along one of the Ni-O bond and x' axis pointing along the Ni-O bond approximately perpendicular to it.) (c) Plot of effective Ni $y'z'$ Wannier functions. Plotted are the orbital shapes (constant-amplitude surfaces) with the lobes of opposite signs colored as red (light gray) and blue (dark gray). The upper two panels correspond to calculations in the equilibrium (left panel) and Ni displaced (right panel) conditions in the ferromagnetic phase, while the lower panels correspond to calculations in the equilibrium (left panel) and Ni displaced (right panel) conditions in the ferrimagnetic phase. The arrows marked in the Wannier functions in the ferromagnetic phase show the sense of rotation of the orbital tails.

the ferromagnetic phase having a spread of ≈3.6 Å compared to that in the ferrimagnetic phase, having a spread of ≈2.7 Å. This is due to the fact that [cf. Fig. 1(b)] Mn t_{2g} states are close in energy to Ni t_{2g} down-spin states ($\Delta \approx 1.6$ eV) in the ferromagnetic phase while Mn t_{2g} states are farther away from Ni t_{2g} up-spin states ($\Delta \approx 2.6$ eV) in the ferrimagnetic phase, resulting in stronger Ni-Mn hybridization in the ferromagnetic phase.

As the angle Ni-O-Mn increases in one quadrant and decreases in the opposite quadrant upon displacement of Ni atom [cf. Fig. 2(a)], oxygen-Mn bonding along the tails strengthens along one direction and weakens along the opposite direction implying a net transfer of charge. The most striking and key observation is that in addition to the net charge-transfer effect, the Mn t_{2g}-like tails rotate in quadrants that show accumulation of charge [see Fig. 2(c)]. This mechanism is different from the charge transfer along a line through unit cell, and gives a shift in the center of Wannier function along y ($-x$) direction when Ni atom is off-centered along x (y) direction. The center of gravity of Wannier function with 1% displaced Ni atom along x direction shows a net displacement of about 0.05 Å along y direction, which is about 1.5% of the lattice constant. Thus, this is responsible for the large off-diagonal component of the Z^* tensor of Ni. Change in the alignment of Ni and Mn spins from FM to FiM leads to weaker hybridization between Ni and Mn, and hence a much smaller antisymmetric component of the Z^*. Examination of BEC tensor shows diagonal component of Mn to be more anomalous compared to that of Ni, which is explained in terms of the dynamical charge transport from/to oxygen atoms. Mn being in d^3 state, is more d^0 like compared to Ni, which is in d^8 state. Using simple criterion of capacity of an orbital available to exchange charge with O^{2-}, one finds that the maximum permitted values for Ni^{2+} in d^8 state is +2, and that for Mn^{3+} in d^3 state is +5, allowing for a maximum value of BEC of +4 and +8 for Ni and Mn, respectively.

V. COMPARISON WITH OTHER COMPOUNDS

$LiNbO_3$, very similar in structure with rhombohedral symmetry to LNMO, was also reported[20] to exhibit a large antisymmetric component of Born charge tensor of Nb. As Nb is in the d^0 state in $LiNbO_3$, following the orbital filling criterion, the magnitude of the diagonal components of Z^*_{Nb} (8.3) is much larger than the off-diagonal ones (2.1), in contrast to LNMO. Due to symmetry, the antisymmetric components of $Z^\star$ of two Nb ions in $LiNbO_3$ are opposite in sign and cancel, in contrast to very disparate magnitudes of the antisymmetric components of $Z^\star$ of Ni and Mn in LNMO. The band-by-band decomposition technique[18] for analysis of Z^* in case of LNMO reveals that the antisymmetric component of $Z^*=3.2$ of Ni arises primarily from O p and metal $3d$ states with contributions of 5.5 and −1.8, respectively, confirming once again the role of the metal (Mn) $3d$ states. In comparison, the antisymmetric charge of 2.1 for Nb in $LiNbO_3$ is mostly contributed by oxygen p states. Importantly, Nb being in d^0 state does not exhibit the interesting effects of magnetic nature as observed for LNMO. Referring to Table I and comparing with Table VI in Ref. 20 we make the interesting observation that upon changing the magnetic ordering from FM to FiM in La_2NiMnO_6, the behavior to the Z^* matrix becomes more akin to $LiNbO_3$, with nearly symmetric off-diagonal components of Z^* at oxygen sites and nearly similar antisymmetric off-diagonal components of Z^* between Ni and Mn (in case $LiNbO_3$ they are identical between two Nb ions in the unit cell due to symmetry). Presence of large off-diagonal elements of Z^* have been also observed for relaxor $PbMg_{1/3}Nb_{2/3}O_3$,[11] but like $LiNbO_3$ it also does not show the interesting effects of magnetic nature.

While the symmetry of the structure allows antisymmetric Born charge in LNMO, its magnitude depends on the energies of the d orbitals and hence on the type of magnetic ordering. Being motivated by this finding, we determined the Born effective charges of another insulating double perovskite, namely, Sr_2CrOsO_6,[21] which also has a rhombohedral symmetry in certain temperature range. Though, we observe antisymmetric off-diagonal Born effective charges at O s site, driven by the symmetry of the rhombohedral phase, its magnitude is found to be much smaller (≈0.3). The observed

case in LNMO is therefore a rare event where the geometry, chemistry, and magnetism work hand-in-hand to produce such a spectacular effect.

VI. SUMMARY AND OUTLOOK

In summary, we have provided a first-principles theoretical evidence for a magnetism-dependent electrostructural coupling in La_2NiMnO_6: it exhibits an anomalously large antisymmetric component of the BEC matrix that depends sensitively on the magnetic order. Fundamental understanding developed here in terms of aspects of symmetry and electronic structure responsible for the fascinating properties of La_2NiMnO_6 should stimulate further efforts in designing new materials exhibiting magnetism-dependent electrostructural coupling. This would lead to changes in the intensity of the IR spectra upon application of magnetic field as well as rotation of the plane of vibration of Ni upon shining a plane-polarized IR radiation, with respect to the plane of polarization of the incident IR radiation.

ACKNOWLEDGMENTS

We thank David Vanderbilt, Nicola Spaldin, and Arup Raychaudhuri for fruitful discussions. T.S.D. acknowledges the financial support through Swarnajayanti and advanced materials research unit. T.S.D. also thanks the hospitality of ICMR, Santa Barbara during which the manuscript was prepared. D.D.S. acknowledges support of J. C. Bose grants. U.V.W. thanks Center for Computational Materials Science, JNCASR for financial aid, and SNBNCBS for kind hospitality.

*waghmare@jncasr.ac.in
†tanusri@bose.res.in

[1] J. Hemberger, P. Lunkenheimer, R. Fichtl, H.-A. Krug von Nidda, V. Tsurkan, and A. Loidl, Nature (London) **434**, 364 (2005).
[2] T. Kimura, S. Kawamoto, I. Yamada, M. Azuma, M. Takano, and Y. Tokura, Phys. Rev. B **67**, 180401(R) (2003).
[3] M. Azuma, K. Takata, T. Saito, S. Ishiwata, Y. Shimakawa, and M. Takano, J. Am. Chem. Soc. **127**, 8889 (2005).
[4] N. S. Rogado, J. Li, A. W. Sleight, and M. A. Subramanian, Adv. Mater. **17**, 2225 (2005).
[5] D. J. Singh and Chul Hong Park, Phys. Rev. Lett. **100**, 087601 (2008).
[6] H. Das, U. V. Waghmare, T. Saha-Dasgupta, and D. D. Sarma, Phys. Rev. Lett. **100**, 186402 (2008).
[7] M. Born and K. Huang, *Dynamical Theory of Crystal Lattices* (Oxford University Press, Oxford, 1968).
[8] W. Zhong, R. D. King-Smith, and D. Vanderbilt, Phys. Rev. Lett. **72**, 3618 (1994).
[9] Ph. Ghosez, J.-P. Michenaud, and X. Gonze, Phys. Rev. B **58**, 6224 (1998).
[10] S. Massidda, M. Posternak, A. Baldereschi, and R. Resta, Phys. Rev. Lett. **82**, 430 (1999).
[11] N. Choudhury, R. E. Cohen, and E. J. Walter, Comput. Mater. Sci. **37**, 152 (2006).
[12] X. Gonze (http://www.abinit.org).
[13] J. P. Perdew, K. Burke, and M. Ernzerhof, Phys. Rev. Lett. **77**, 3865 (1996).
[14] O. K. Andersen and T. Saha-Dasgupta, Phys. Rev. B **62**, R16219 (2000).
[15] E. Pavarini, I. Dasgupta, T. Saha-Dasgupta, O. Jepsen, and O. K. Andersen, Phys. Rev. Lett. **87**, 047003 (2001).
[16] T. Saha-Dasgupta, Molly De Raychaudhury, and D. D. Sarma, Phys. Rev. Lett. **96**, 087205 (2006).
[17] T. Saha-Dasgupta, R. Valenti, F. Capraro, and C. Gros, Phys. Rev. Lett. **95**, 107201 (2005).
[18] P. Ghosez and X. Gonze, J. Phys.: Condens. Matter **12**, 9179 (2000).
[19] Alessio Filippetti and Nicola A. Hill, Phys. Rev. B **65**, 195120 (2002).
[20] M. Veithen and Ph. Ghosez, Phys. Rev. B **65**, 214302 (2002).
[21] H. Das, M. De-Raychaudhury, and T. Saha-Dasgupta, Appl. Phys. Lett. **92**, 201912 (2008).